A New Simplified Parameterization of Secondary Organic Aerosol in the Community Earth System Model Version 2 (CESM2; CAM6.3)

Duseong S. Jo[1], Simone Tilmes[1], and Louisa K. Emmons[1], Siyuan Wang[2,3], Francis Vitt[1]

[1]National Center for Atmospheric Research, Boulder, CO, USA
[2]Cooperative Institute for Research in Environmental Sciences, University of Colorado, Boulder, CO, USA
[3]NOAA Chemical Sciences Laboratory, Boulder, CO, USA

Correspondence to: Duseong S. Jo (cdswk@ucar.edu)

Manuscript submitted to Geoscientific Model Development

9   **Abstract.** The Community Earth System Model (CESM) community has been providing versatile

10 modeling options, with simple to complex chemistry and aerosol schemes in a single model, in order to

11 support the broad scientific community with various research interests. While different model

12 configurations are available in CESM and these can be used for different fields of Earth system science,

13 simulation results that are consistent across configurations are still desirable. Here we develop a new

14 simple secondary organic aerosol (SOA) scheme in the Community Atmosphere Model version 6.3

15 (CAM6.3), the atmospheric component of the CESM. The main purpose of this simplified SOA scheme

16 is to reduce the differences in aerosol concentrations and radiative fluxes between CAM and CAM with

17 detailed chemistry (CAM-chem) while maintaining the computational efficiency of CAM. CAM

18 simulation results with the current and the new SOA schemes are compared to the CAM-chem results as

19 a reference. More consistent SOA concentrations are obtained globally when using the new SOA

20 scheme, for both temporal and spatial variabilities. Furthermore, the overestimation of other

21 carbonaceous aerosols (black carbon and primary organic aerosol) in CAM is greatly reduced, which

22 results in improved global atmospheric burden and concentrations at the high latitudes of the Northern

23 Hemisphere compared to the full chemistry version (CAM-chem). As a result, the high bias of radiative

24 flux in the Arctic region is significantly reduced for both nudged and free-running simulations. We find

25 that the current SOA scheme in CAM can still be used for radiative forcing calculation as the high

26 biases exist both in pre-industrial and present conditions, but studies focusing on the instantaneous

27 radiative effects would benefit from using the new SOA scheme. The new SOA scheme also has

28 technical advantages including the use of identical SOA precursor emissions as CAM-chem from the

29 online biogenic emissions, instead of pre-calculated emissions that may introduce differences. Future

30 parameter updates on the CAM-chem SOA scheme can be easily translated to the new CAM SOA

31 scheme as it is derived from the CAM-chem SOA scheme.

32   **Short Summary**. The new simple secondary organic aerosol (SOA) scheme has been developed for the

33   Community Atmosphere Model (CAM), based on the complex SOA scheme in CAM with detailed

34   chemistry (CAM-chem). The CAM with the new SOA scheme shows better agreements with

35   CAM-chem in terms of aerosol concentrations and radiative fluxes, which ensures more consistent

36   results between different compsets in the Community Earth System Model. The new SOA scheme also

37   has technical advantages for future developments.

1 Introduction

Secondary organic aerosol (SOA) accounts for a substantial fraction of ambient tropospheric aerosol (Hallquist et al., 2009). Atmospheric models generally use parameterizations to simulate SOA because it is composed of a wide range of different organic molecules (Goldstein and Galbally, 2007). The SOA parameterization in atmospheric chemistry models varies from the simple method of multiplying constant yields to emissions, to the complex volatility basis set (VBS) approach, which considers the oxidation of volatile organic compounds (VOCs) and gas-particle partitioning, as shown in the recent model intercomparison study for organic aerosol (OA) (Hodzic et al., 2020).

Climate models that have to perform hundreds of years of simulations and many ensemble members often use very simple parameterizations to calculate SOA in the model (Tsigaridis and Kanakidou, 2018), due to the high computational cost associated with chemistry, deposition, and the increased number of model tracers to be transported (Jo et al., 2019). Because SOA affects climate through aerosol-radiation and aerosol-cloud interactions, and climate also affects SOA through changing biogenic emissions and photochemistry (Gettelman et al., 2019a; Sporre et al., 2019; Tilmes et al., 2019; Jo et al., 2021), the accurate representation of SOA in climate models is important but needs to have low computational cost for long-term simulation purposes.

The Community Earth System Model Version 2 (CESM2) has two different SOA schemes, one simplified scheme for the Community Atmosphere Model version 6 (CAM6) (Danabasoglu et al., 2020) and the Whole Atmosphere Community Climate Model version 6 (WACCM6) with the Middle Atmosphere (MA) chemistry (Gettelman et al., 2019b), and a VBS scheme for the CAM6 with comprehensive chemistry (CAM6-chem) (Emmons et al., 2020) and the WACCM6 with the TSMLT (troposphere, stratosphere, mesosphere, and lower thermosphere) mechanism. For the purpose of climate studies using many ensemble members, CAM6 is generally used for computational efficiency. Models like WACCM6 with TSMLT are used for detailed chemistry and aerosol studies, but in general, only a few ensemble members can be performed. Ideally, the two SOA schemes in simple and complex chemistry configurations should give the same results to maintain model consistency regarding aerosol fields and resulting climate forcings, but the spatial and temporal distributions of SOA between CAM

65 and CAM-chem (and WACCM TSMLT) are different enough to have a significant effect on black

66 carbon (BC) and the Earth's radiation budget (Tilmes et al., 2019).

67   Here we propose a new simplified and computationally affordable SOA scheme for CAM, which is

68 based on the VBS scheme in CAM-chem. We compare three SOA schemes (VBS, current simplified

69 SOA, and new simplified SOA) under a few different CESM2 configurations (specified dynamics and

70 free-running in preindustrial and present conditions). The new approach substantially reduces the

71 differences in aerosol and radiation values between CAM and CAM-chem (Sect. 3). The new SOA

72 scheme also has a technical advantage as it does not need input files for the SOA precursor, but uses the

73 same emissions files as CAM-chem or WACCM for individual SOA precursor species (isoprene,

74 terpenes, toluene, etc.).

75 **Table 1.** SOA schemes used in this study. Computational costs are estimated on the Cheyenne
76 supercomputer at NCAR. Computational cost ranges are given in parentheses with the average value.

SOA scheme	CAM-chem	CAM	CAM (NEW)
Emissions	Individual VOCs, online biogenic emissions	Pre-calculated, lumped SOAG emissions	Individual VOCs, online biogenic emissions
VOCs and chemistry	explicitly simulated	No	Lumped tracer (SOAE) with 1-day lifetime
Number of SOA bins	5	1	1
Saturation vapor pressure	0.01 , 0.1, 1, 10, 100	1.02	1
Enthalpy of vaporization	153, 142, 131, 120, 109	156	131
SOA yield	Based on the VBS	Fixed fraction and scaled up by 50%	Based on the VBS but lumped
Loss processes	wet & dry deposition of SOAG photolytic loss of SOA	No deposition of SOAG No photolytic loss	wet & dry deposition of SOAG photolytic loss of SOA
Computational cost (pe-hrs / simulated_year)	7933 (7783 - 8083)	2398 (2353 - 2448)	2455 (2414 - 2501)

2 Method

In this section, we present SOA schemes in CAM-chem and CAM, along with the new simplified SOA scheme, as summarized in Fig. 1 and Table 1. General descriptions for other carbonaceous aerosols (BC and primary organic aerosol (POA)) are also explained as concentrations of those carbonaceous aerosols are affected by SOA concentrations (Tilmes et al., 2019). This section also includes the simulation set-up for comparisons between SOA schemes in Sect 3.
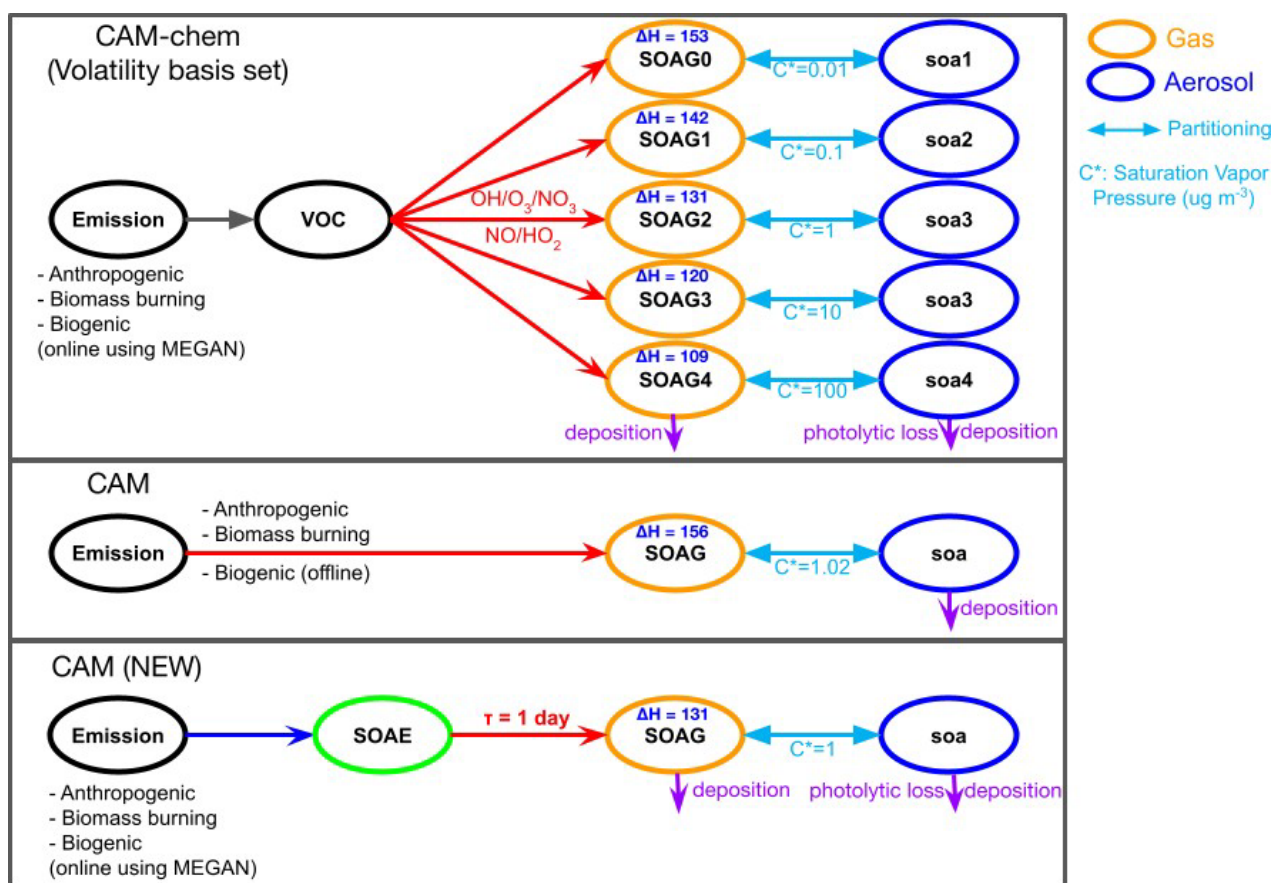
Figure 1. Schematic diagrams of SOA parameterizations in CESM2.

Geoscientific
Model Development
Discussions

2.1 SOA scheme in CAM-chem

SOA in CAM-chem is simulated using the VBS approach, as described by Tilmes et al. (2019). The VBS scheme in CAM-chem incorporates recent findings such as wall-corrected SOA yields, photolytic removal of SOA, and more efficient removal by dry and wet deposition. Details can be found in Hodzic et al. (2016). Here we briefly describe the characteristics that can be compared to the simple SOA scheme in CAM.

CAM-chem uses a VBS scheme with 5 volatility bins (see Fig. 1) with saturation vapor pressures spanning from 0.01 to 100 $\mu g\ m^{-3}$ at 300K. Enthalpy of vaporization values are 153, 142, 131, 120, and 109 $kJ\ mol^{-1}$ for 0.01, 0.1, 1, 10, and 100 $\mu g\ m^{-3}$, respectively, at 300K based on Epstein et al. (2010). Traditional SOA precursors such as isoprene, monoterpenes, sesquiterpenes, benzene, toluene, and xylenes are explicitly simulated in the model, and the oxidation of those VOCs with OH, O_3, and NO_3 makes gas phase intermediate precursors of SOA (SOAG) according to the volatility bins. Semi- and intermediate-range volatility organic compounds (S/IVOCs) are also considered with a simple OH reaction. Since S/IVOCs are defined by volatility and exact chemical speciation is not available for them, 60% of POA and 20% of total non-methane VOC (NMVOC) emissions are assumed to be SVOCs and IVOCs, respectively (Hodzic et al., 2016). Biogenic VOCs are calculated online using the model of emissions of gases and aerosols from nature version 2.1 (MEGAN2.1) (Guenther et al., 2012) available in the Community Land Model version 5 (CLM5), a component of CESM and coupled to CAM (Lawrence et al., 2019). CAM-chem also supports an extended VBS compset that keeps track of VBS tracers from three sources (anthropogenic, biomass burning, and biogenic), leading to 15 SOA species simulated in total. This option is not generally used except for studies tracking sources of SOA, as total SOA burden and formation are very similar between the two options because the same volatility bins are used (Tilmes et al., 2019).

In terms of aerosol modes, the four-mode version of the Modal Aerosol Module (MAM4) is generally used in recent scientific applications (Liu et al., 2016). MAM4 considers Aitken, accumulation, coarse, and primary carbon modes. SOA is simulated using Aitken and accumulation modes but most of the mass (>99%) is in the accumulation mode (Tilmes et al., 2019). In total, 15

127 tracers (5 for the gas phase and 10 for the aerosol phase - 5 bins × 2 modes) are used for the SOA

128 calculation in CAM-chem.

2.2 Current SOA scheme in CAM

130 The current simplified SOA scheme in CAM uses 3 tracers (1 for the gas phase and 2 for the

131 aerosol phase). Like the VBS, both gas-phase (SOAG) and aerosol-phase (soa_a1 and soa_a2 for

132 accumulation and Aitken modes) are simulated with gas-aerosol partitioning, with the enthalpy of

133 vaporization of 156 kJ mol^{-1} and the saturation vapor pressure of 1.02 μg m^{-3} (Liu et al., 2012). SOAG

134 does not undergo dry and wet removal, which is also different from the VBS that calculates dry and wet

135 deposition of gas-phase semivolatiles.

136 Unlike the VBS representation which explicitly simulates parent VOCs, this scheme does not

137 simulate the chemistry of VOCs but uses pre-calculated emissions using fixed mass yields for the

138 following VOC categories: 5% BIGALK (lumped ≧C4 alkanes), 5% BIGENE (lumped ≧C4 alkenes),

139 15% aromatics, 4% isoprene, and 25% monoterpenes (Liu et al., 2012). For biogenic VOCs, offline

140 emissions are precalculated and provided as an additional input file based on biogenic emissions

141 simulated by CLM-MEGAN2.1. Generally, the offline biogenic VOC emission does not have annual

142 variations and is repeated over the simulation period. Note that those SOAG emissions are further

143 increased by 50% after model tuning involving aerosol indirect effect (Liu et al., 2012).

2.3 New SOA scheme in CAM

145 The new SOA scheme uses a similar approach to the current SOA scheme in CAM, but several

146 modifications have been made to allow more consistent results with the VBS scheme in CAM-chem.

147 First, VOC species that generate SOA are matched to the VBS. In other words, BIGALK and BIGENE

148 are no longer used for the calculation of SOA emissions, and instead, sesquiterpenes and S/IVOCs are

149 considered for calculating the interactive emissions of SOA. This change can be scientifically justified

150 because SOA yields increase with the carbon number (Srivastava et al., 2022). BIGALK and BIGENE

151 are mainly composed of C4-C6 alkanes and alkenes (Emmons et al., 2020), but S/IVOCs correspond to

152 C12 or higher n-alkanes (Robinson et al., 2007).

153   Second, SOA yields (used for the interactive emissions) have been calculated based on the VBS

154   yields in CAM-chem. SOA yields for the first four bins and 20% of the fifth bin are summed up for

155   each compound. Only 20% of the fifth bin yield is used, as it is the most volatile bin. We consider SOA

156   yields from OH reactions only in this calculation, because reaction with OH is dominant for VOCs.

157   Only low NO_x yields are used in this study which is consistent with Tilmes et al. (2019), which is

158   appropriate for global climate studies with 1° horizontal resolution of the model grid. For air quality

159   studies with high spatial resolution, CAM-chem with NO_x-dependent SOA yields can be used

160   (Schwantes et al., 2022). The resulting SOA yields derived from CAM-chem results are 0.28, 0.64,

161   0.04, 0.16, 0.45, 0.35, 0.41, and 0.80 for monoterpenes, sesquiterpenes, isoprene, benzene, toluene,

162   xylenes, IVOC, and SVOC, respectively. Those are constants and do not change during the run, like

163   SOA yields used in the VBS scheme. It is worth noting that those yields can be easily updated in the

164   CAM run-time namelist file if there is a future update to the CAM-chem VBS scheme.

165   Third, we add a new tracer called "SOAE" (Fig. 1) to consider the time that VOCs and intermediate

166   chemical species undergo oxidation before forming semivolatiles. We assume a constant 1-day e-folding

167   lifetime to convert "SOAE" to "SOAG" which can be partitioned into aerosols so that oxidant fields do

168   not have to be simulated in CAM for computational efficiency. The 1-day lifetime corresponds to the

169   OH reaction rate constant of 10^{12} cm^3 $molecules^{-1}$ s^{-1} with a global annual mean OH concentration of

170   11.6×10^5 $molecules$ cm^{-3} (Warneck and Williams, 2012).

171   Fourth, parameters are adjusted for consistency with the VBS scheme. The enthalpy of vaporization

172   is changed from 156 to 131 kJ mol^{-1}, which is the value used in the third bin of the VBS scheme. This

173   can change SOA in the upper troposphere where temperature dependency becomes important.

174   Deposition of gas phase SOA (SOAG) and the photolytic reaction of SOA are also added, which can

175   affect SOA concentrations in the remote atmosphere. Saturation vapor pressure change with the

176   assumption of 10% of POA as oxygenated (Liu et al., 2012) is not used in this scheme for consistency

177   with the VBS scheme.

178   Fifth, the same offline emission files (anthropogenic and biomass burning) and online emission

179   (biogenic) are used as the VBS method, via namelist control. As a result, preprocessing for SOAG

180   emission is no longer needed, and annual variability as well as the diurnal cycle for biogenic emission

can be easily considered. Note that biogenic emission is always calculated in CLM, regardless of whether the emission is used or not in CAM or CAM-chem. Therefore, using online biogenic emissions does not add computational cost.

2.4 Other carbonaceous aerosols

Here we describe BC and POA simulations in CAM and CAM-chem, as those are affected by SOA concentrations through microphysics. Because BC, POA, and SOA precursors are emitted from the same sources (except for the biogenic SOA) and share the same aerosol mode (accumulation mode), changes in one component can significantly affect other components. Tilmes et al. (2019) reported ~20% differences between the simplified SOA and the VBS scheme in terms of the global burden of BC and POA, while the difference for the sulfate burden was very small (< 1%).

Unlike SOA, there is no difference in BC and POA simulation schemes between CAM and CAM-chem, because BC and POA are chemically inert and the standard aerosol module is the same (MAM4) for both CAM and CAM-chem. BC and POA are emitted into the primary carbon mode (bc_a4 and pom_a4) and are transferred to the accumulation mode (bc_a1 and pom_a1) through microphysical aging (Liu et al., 2016). The aging rate is substantially affected by SOA, through changing internally mixed aerosol numbers (Tilmes et al., 2019).

2.5 Simulation set-up

We conduct three types of model experiments for different application scenarios using the development version of CESM2.2 or CAM6.3 (tag name: cam6_3_050). First, a specified dynamics run is performed for the analysis of the present condition using the nudged meteorological fields. Temperature and horizontal winds are nudged towards the Modern-Era Retrospective analysis for Research and Applications version 2 (MERRA2) every 3 hours (Gelaro et al., 2017). In this simulation, we run the model for the year 2013 with a spin-up period of one year. Second, historical runs are performed for the 1850s and 2000s with prescribed sea surface temperatures and sea ice conditions. These are free-running simulations for 12 years for each condition with the two years discarded for the spin-up. In this case, the CLM is run with the satellite phenology (SP) option which uses a prescribed

207 leaf area index (LAI) based on MODIS satellite observations (Lawrence et al., 2019). In this option, the

208 input LAI value for each plant functional type (PFT) is the same between the 1850s and 2000s but the

209 PFT fraction changes with time. As a result, the final LAI used for biogenic emission calculation is

210 slightly different between the two periods. The third is the same as the second experiment, but the

211 vegetation state including LAI is simulated prognostically by CLM (biogeochemistry; BGC) (Lawrence

212 et al., 2019). In addition to absolute values, the difference between the 1850s and 2000s is investigated

213 from the historical simulations in Sect. 3.3, to compare simulation results in terms of the radiative

214 forcing. In all simulations, the bi-directional oceanic flux of dimethyl sulfide (DMS) is calculated using

215 the Online Air-Sea Interface for Soluble Species (OASISS) (Wang et al., 2019, 2020) and the

216 climatological surface seawater DMS concentration (Lana et al., 2011), which will be the default DMS

217 emission in the next CESM version (CAM7).

3 Results

219 In this section, the current and new SOA schemes in CAM are evaluated against CAM-chem as a

220 reference. As SOA changes can affect the other carbonaceous aerosols and radiation fields in CESM2

221 (Tilmes et al., 2019), we also compare those simulation fields as shown in Table 2.

3.1 Aerosols

223 Table 2 shows the global annual mean burden of aerosols by different simulations, including

224 gas-phase SOA or semivolatiles (SOAG). Two CAM cases and CAM-chem are consistent within 10%

225 in terms of global SOA burden, with the new scheme showing better agreement. gas-phase SOA

226 (SOAG) is substantially underestimated in both CAM cases, because high volatility bins (saturation

227 vapor pressure of 10 µg m^{-3} and 100 µg m^{-3}) are not simulated in the 1-bin simple SOA scheme.

228 However, SOAG does not affect other aerosol concentrations and radiation fields, and therefore it is not

229 an important species in CAM.

Table 2. Global annual mean burden of carbonaceous aerosols (SOA, SOAG (SOA in the gas phase), BC, and POA) and radiation fields (FSNT (net shortwave flux at top of model), FLNT (net longwave flux at top of model), top of the atmosphere (TOA) imbalance, SWCF (shortwave cloud forcing), LWCF (longwave cloud forcing)). Because CAM uses the offline biogenic SOA emissions, SOA in the default CAM is not affected by the CLM option (Sect. 2.5). Units are Gg for aerosols and W m^{-2} for radiation fields.

Simulation	SOA scheme	SOA	SOAG	BC	POA	FSNT	FLNT	TOA imbalance	SWCF	LWCF
2013 (Nudged)	CAM-chem	1022	484	117	587	236.7	238.7	-2.0	-50.5	22.2
	CAM	948	118	131	704	237.7	239.2	-1.5	-49.6	21.7
	CAM (NEW)	1027	129	111	574	237.3	239.3	-2.0	-49.8	21.6
1850s (SP)	CAM-chem	780	367	31	299	232.3	235.0	-2.7	-54.6	26.3
	CAM	699	102	43	435	233.1	235.4	-2.3	-53.7	25.7
	CAM (NEW)	747	94	30	300	232.7	235.3	-2.7	-54.0	25.7
2000s (SP)	CAM-chem	793	375	89	510	231.3	234.0	-2.7	-56.1	25.7
	CAM	796	102	102	635	232.0	234.4	-2.4	-55.3	25.1
	CAM (NEW)	744	105	83	488	231.7	234.4	-2.7	-55.6	25.1
1850s (BGC)	CAM-chem	826	357	31	302	232.2	235.0	-2.8	-55.0	26.4
	CAM (NEW)	770	89	31	304	232.6	235.3	-2.7	-54.3	25.9
2000s (BGC)	CAM-chem	982	411	88	510	231.3	234.0	-2.7	-56.3	25.8
	CAM (NEW)	952	109	83	490	231.6	234.3	-2.7	-55.8	25.2
2000s - 1850s (SP)	CAM-chem	13	8	57	210	-0.98	-0.97	-0.01	-1.47	-0.54
	CAM	97	0	60	200	-1.15	-1.04	-0.11	-1.67	-0.66
	CAM (NEW)	-3	11	52	188	-0.98	-0.91	-0.07	-1.58	-0.70
2000s - 1850s (BGC)	CAM-chem	156	54	57	208	-0.92	-1.08	0.16	-1.31	-0.59
	CAM (NEW)	182	19	52	185	-0.96	-0.97	0.01	-1.44	-0.75

260   Although two CAM cases show similar global SOA burdens to CAM-chem, their temporal and
261   spatial distributions are very different. Figure 2 shows the monthly timeseries and mean vertical profile
262   of the global SOA burden simulated by CAM and CAM-chem in 2013. The SOA underestimation
263   during the northern hemisphere winter time and the SOA build-up in the upper atmosphere (< 100 hPa)
264   are greatly improved in the new CAM SOA scheme. There is still a discrepancy between the new CAM
265   and CAM-chem such as SOA at around 500 hPa and at the surface (Fig. 2d), due to the limitation of
266   using only one volatility bin in CAM (to reduce the computational cost). One fixed volatility bin with
267   one enthalpy value cannot fully reproduce gas-phase semivolatiles simulated by five bins and the
268   temperature dependency of volatility changes.
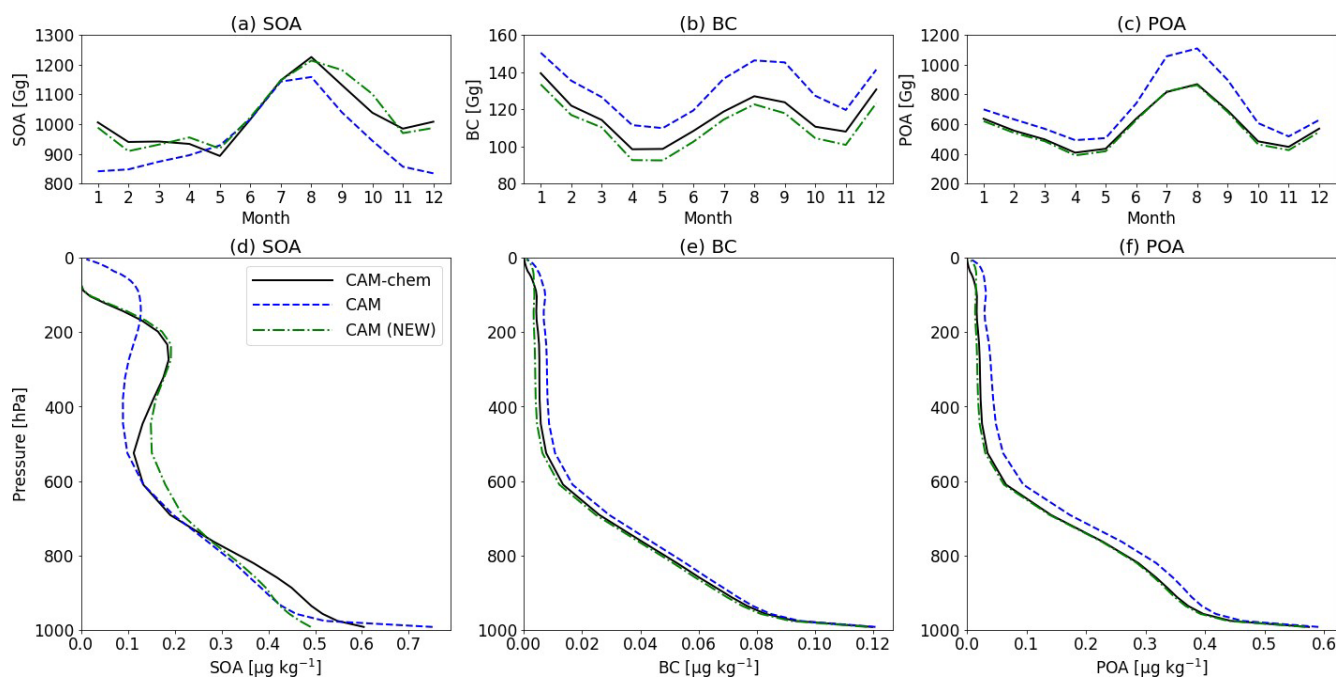

269   **Figure 2.** Monthly timeseries of global atmospheric burden (first row) and vertical distributions (second
270   row) of annual average SOA, BC, and POA simulated by CESM2.

271   Figure 3 shows the global spatial distribution of SOA at 100 hPa, 500 hPa, 850 hPa, and the surface

272   levels simulated by CAM-chem and CAM. In the current CAM simulation, the main source regions

273   (South America and Africa) are well represented at the surface layer (Fig. 3k) but do not appear in the

274   free troposphere and above (panels b, e, and h). This is because the current CAM SOA scheme

275   generates semivolatiles directly from the surface emissions while the CAM-chem SOA scheme needs

276   more time for VOC reactions to make semivolatiles, which can form SOA in the free troposphere. The

277   intermediate tracer (SOAE) in the new CAM implicitly considers this process and successfully captures

278   SOA peaks in the free troposphere (panels c, f, and i).

279   In addition, the current CAM fails to reproduce the sharp gradient of CAM-chem SOA above 200

280   hPa (Fig. 2d) and simulates too much SOA globally (Fig. 3b). The missing loss processes (deposition of

281   semivolatiles and photolytic loss of SOA) and higher temperature dependency (enthalpy) of saturation

282   vapor pressure result in more SOA in the current CAM simulation. This problem is solved in the new

283   CAM SOA scheme (Fig. 3c).

284   Significant improvements are also found for BC and POA. The current CAM simulates up to ~45%

285   differences while the new CAM shows up to ~7% differences for BC and POA (Table 2). Unlike SOA,

286   seasonalities of BC and POA are well represented in the current CAM (panels b and c in Fig. 2), since

287   BC and POA schemes are the same between CAM and CAM-chem. Spatial distributions are also

288   similar (Figs. S2–S5) except for the Arctic regions in the upper atmosphere. This difference can

289   significantly affect the radiation budget in the Arctic region (Sect. 3.2), which should be important for

290   climate studies focusing on the Arctic.
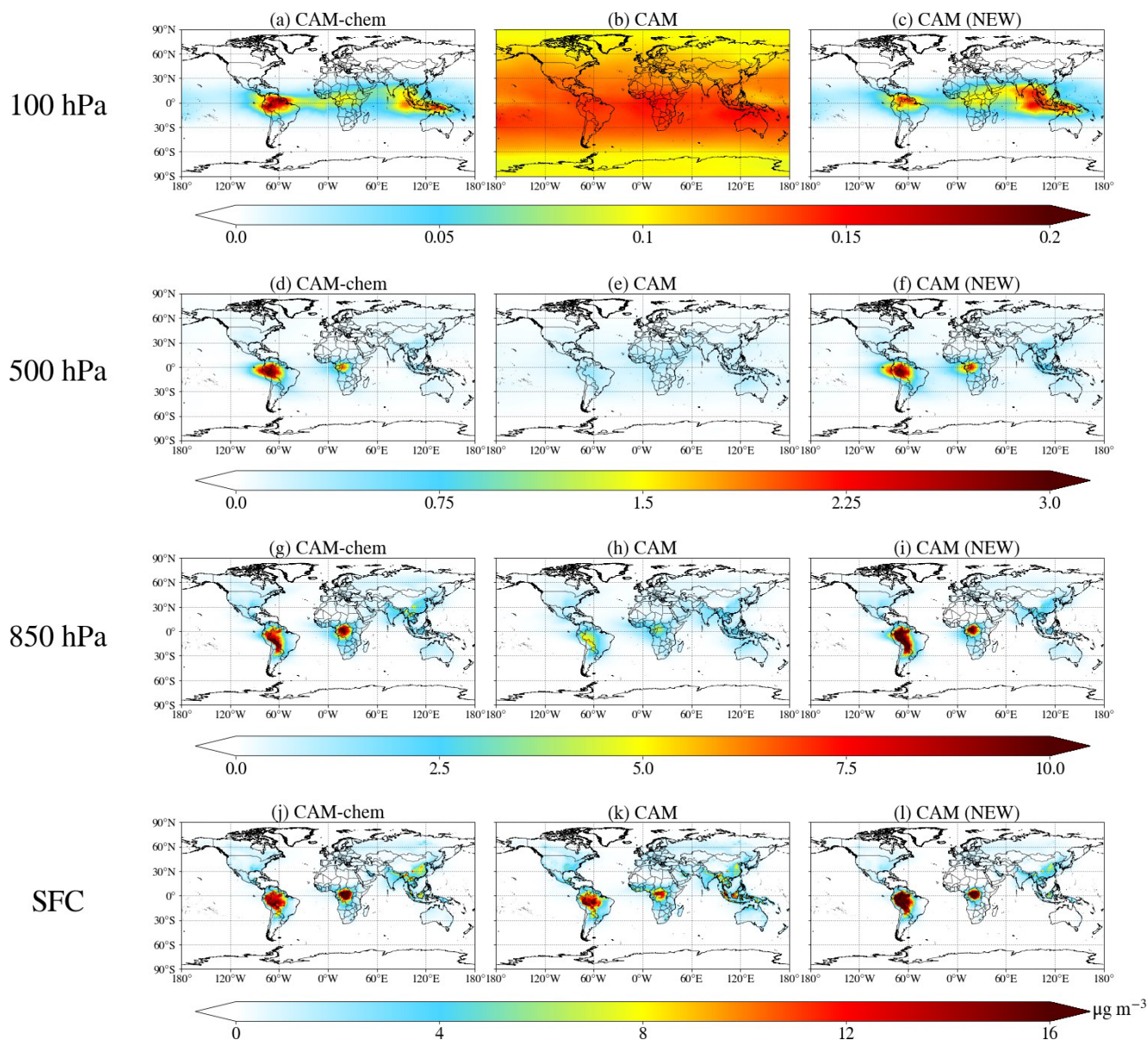
Figure 3. Global maps of SOA concentrations in 2013 simulated by CAM-chem (first column), CAM (second column), and CAM (NEW) (third column) at four different vertical levels (surface, 850 hPa, 500 hPa, and 100 hPa). The difference maps between CAM and CAM-chem are available in Fig. S1.

3.2 Radiation fields

294

295   As aerosols can affect radiative fluxes through direct and indirect effects, here we investigate the

296   radiation changes with the new SOA scheme in CAM, in terms of the difference between CAM and

297   CAM-chem. Figure 4 shows the zonal averages of net shortwave (SW) and longwave (LW) fluxes and

298   cloud forcings in CAM compared to CAM-chem. The most notable differences occur in the high

299   latitudes in the Northern Hemisphere, similar to aerosol concentration changes shown in Sect 3.1. Both

300   aerosol-radiation and aerosol-cloud interactions almost equally contribute to the positive bias (panels a

301   and d). This strong positive bias of the SW flux in the current CAM is greatly improved with the new

302   SOA scheme.
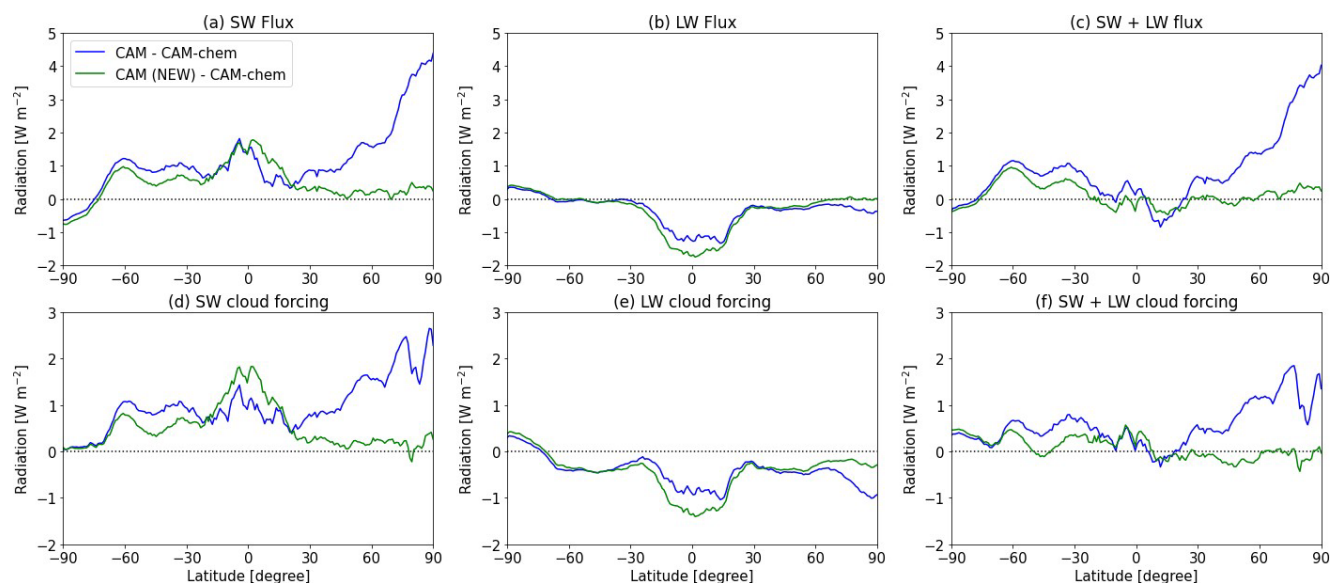
Figure 4. Zonal averages of the radiation difference in 2013 between CAM and CAM-chem. Radiative
fluxes at the top of the model are presented in the first row (a-c) and cloud forcings are shown in the
second row (d-f).

306   Biases are slightly increased over the Tropics when it comes to SW and LW fluxes individually,

307   which are mainly caused by the cloud effects as shown in Figs. 4d and 4e, but those are canceled out in

308   terms of the total radiation (Figs. 4c and 4f). Overall, the new SOA scheme shows slight improvements

309   in other latitudes as well in addition to the Arctic region. The low bias can be further confirmed by

310   global spatial distributions shown in Fig. S6, the new CAM simulation shows fewer biases in most of

311   the locations globally (panels h and i in Fig. S6).

312 3.3 Historical simulations

313   Analogous to the simulation results with nudged meteorology in Sect 3.1 and 3.2, the new SOA

314   scheme produces more consistent results with CAM-chem than the current CAM SOA scheme (Table

315   2), especially for BC and POA burdens that are affected by SOA through microphysics. The new SOA

316   scheme also captures the increased SOA burden in the 2000s compared to the 1850s when using the

317   BGC option, which is mainly caused by increased biogenic VOC emissions (Fig. S7).

318   Figure S7 further shows that interannual variability may not be a significant factor for isoprene

319   emissions on a 10-years time scale, but this would be important for climate studies with more than 100

320   years of simulation time (1850s vs 2000s). The offline emissions used in the default CAM have no

321   interannual variability, thus not accounting for emission response to climate change.

322   The high bias of the SW + LW flux over the Arctic from the nudged meteorology simulations (Fig.

323   4c) is also found in all historical simulations as shown in Fig. 5. The default CAM shows the high bias

324   for both 1850s and 2000s simulations. However, in terms of the difference between the 2000s and

325   1850s, the biases cancel out, and as a result, the difference between CAM and CAM-chem becomes

326   small (Figs. 5c and 5f). This cancellation implies that previous CAM studies focusing on radiative

327   forcing are still valid, as radiative forcing is calculated as present minus preindustrial radiative effects.

328   In terms of global averages (Table 2), the new CAM also shows improvements, especially for

329   shortwave radiation, not only for absolute values but also for the difference between present and

330   pre-industrial simulations.

17

Geoscientific
Model Development
Discussions
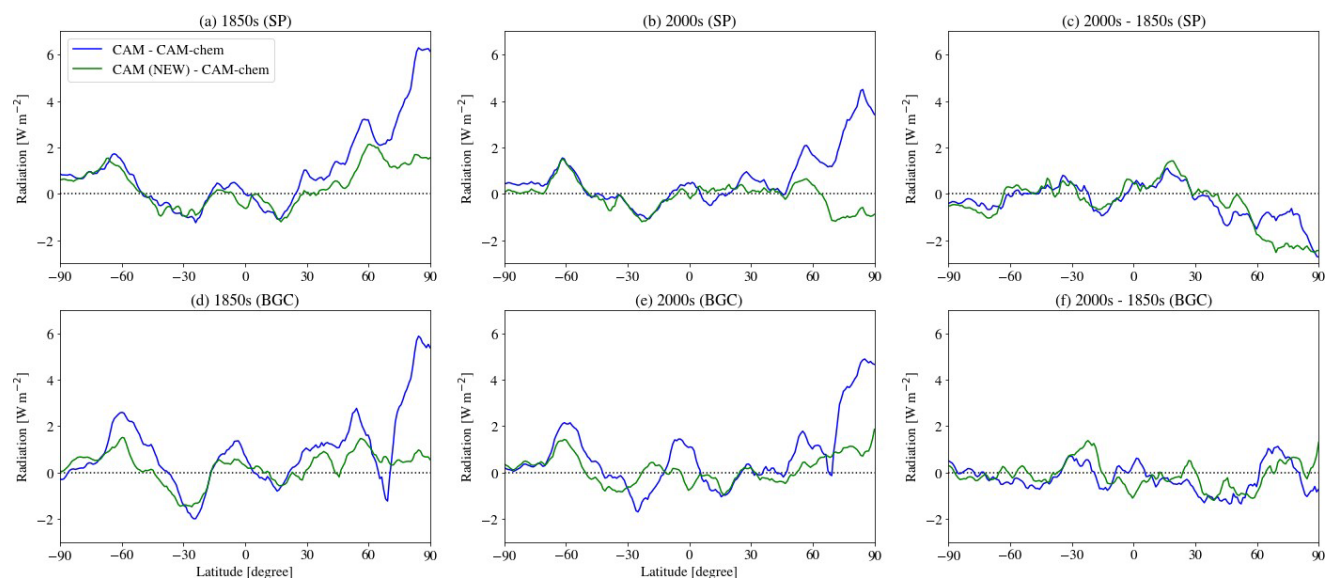
Figure 5. Zonal averages of the SW + LW flux difference in historical simulations (1850s (a and d), 2000s (b and e), and 2000s - 1850s (c and f)) between CAM and CAM-chem. Note that the results from the default CAM simulations are the same for SP and BGC because the default CAM uses offline biogenic emissions. Only CAM-chem results affect the difference between SP and BGC simulations (blue lines).

4 Conclusion and possible future developments of the aerosol scheme in CAM

In this study, we developed a new SOA scheme for use in CAM with simple chemistry. This new SOA scheme was designed to close the gap between CAM and CAM-chem in terms of aerosols and radiative effects while maintaining computational efficiency. The new SOA scheme was derived based on the parameters used in the VBS scheme in CAM-chem, without changing the overall architecture of the simple SOA scheme in the current CAM. As a result, the computational cost remained almost the same with the new SOA scheme (within the range of computing environment variability).

CAM simulation results with the current and new SOA schemes were investigated in terms of carbonaceous aerosols and radiative fluxes. There was no significant bias in terms of the global SOA burden of the current CAM SOA scheme because it was tuned by increasing SOA emissions by 50% (Liu et al., 2012). However, the current CAM SOA scheme was insufficient to reproduce the temporal

18

and spatial (both horizontally and vertically) variabilities of CAM-chem SOA, and the new SOA scheme improved the performance of these variabilities.

The new SOA scheme also improved the simulation of other carbonaceous aerosols (BC and POA) through the microphysics of MAM4. Since BC and POA emissions are the same for all model cases and those aerosols are chemically inert, temporal and horizontal spatial variabilities are generally similar to each other but the absolute concentrations were improved when using the new SOA scheme. The overestimation of BC in CAM was greatly reduced compared to CAM-chem, from ~45% in the current SOA scheme to ~7% in the new SOA scheme. POA is also improved in the same manner. Major improvements were made in the Arctic region for aerosol concentrations in the free troposphere and above.

The improvements in simulating aerosol fields led to more consistent radiative fluxes between CAM and CAM-chem, especially over the high-latitude regions in the Northern Hemisphere. The SW + LW flux at the top of the model was different by up to 6 W m^{-2} and it is persistent regardless of the simulation periods. However, in terms of the radiative forcing which is calculated from the difference between present and pre-industrial conditions, both the current and new CAM simulations showed no significant differences. While the studies investigating the instantaneous radiative effects will need to use the new SOA scheme, the current SOA scheme would still be valid for studies focusing on radiative forcing.

On the practical side, the new SOA scheme has advantages in keeping up with the updates, as it uses the same precursor emissions as the VBS scheme in CAM-chem. The new SOA scheme uses online biogenic emissions as CAM-chem does, therefore the difference between SP and BGC options can be calculated for SOA. If there is a future update in the VBS scheme in CAM-chem, the corresponding updates in CAM can be done easily by changing the namelist file.

Although significant advances have been made in SOA concentration simulation in this study, the aerosol module in CAM still has room for further development. Currently, CAM reads the offline monthly oxidant fields simulated by CAM-chem but oxidants such as OH and O_3 have strong diurnal variations. It would not be computationally feasible for CAM to calculate or read oxidants every hour, but applying constant diurnal profile values to the monthly fields would not add significant

375 computational costs. It may be important for SO_2 oxidation and sulfate formation as well. The formation

376 of SOAG from SOAE is calculated using a 1-day lifetime, but future versions could use the reaction

377 rate constant with OH if the diurnal variation of oxidant fields is introduced in CAM.

378 The new SOA scheme can be further adjusted, for example, for studies focusing on surface aerosol

379 fields, users can easily change SOA yields for different emission sources through namelist changes.

380 Vertical shapes can be also adjusted by changing the parameters such as the enthalpy of vaporization,

381 saturation vapor pressure, and photolysis rates in the future.

382 **Code and data availability.** CESM is an open-source community model and is publicly available at:

383 https://github.com/ESCOMP/CESM. The new SOA scheme is included in the development version of

384 the CAM (https://github.com/ESCOMP/CAM, tag name: cam6_3_093) and will be publicly available in

385 the next CESM release. The model results used in this study are available on the NCAR Digital Asset

386 Service Hub (DASH) at TBD.

387 **Author contributions.** DSJ, ST, and LKE designed the research and developed the SOA scheme. SW

388 developed the OASISS scheme. DSJ, ST, and FV conducted CESM simulations. DSJ wrote the

389 manuscript. All authors contributed to editing the manuscript.

390 **Competing interests.** The authors declare that they have no conflict of interest.

References

398

399 Danabasoglu, G., Lamarque, J. -F, Bacmeister, J., Bailey, D. A., DuVivier, A. K., Edwards, J., Emmons,
400 L. K., Fasullo, J., Garcia, R., Gettelman, A., Hannay, C., Holland, M. M., Large, W. G., Lauritzen, P. H.,
401 Lawrence, D. M., Lenaerts, J. T. M., Lindsay, K., Lipscomb, W. H., Mills, M. J., Neale, R., Oleson, K.
402 W., Otto-Bliesner, B., Phillips, A. S., Sacks, W., Tilmes, S., Kampenhout, L., Vertenstein, M., Bertini,
403 A., Dennis, J., Deser, C., Fischer, C., Fox-Kemper, B., Kay, J. E., Kinnison, D., Kushner, P. J., Larson,
404 V. E., Long, M. C., Mickelson, S., Moore, J. K., Nienhouse, E., Polvani, L., Rasch, P. J. and Strand, W.
405 G.: The community earth system model version 2 (CESM2), J. Adv. Model. Earth Syst., 12(2),
406 doi:10.1029/2019ms001916, 2020.

407 Emmons, L. K., Schwantes, R. H., Orlando, J. J., Tyndall, G., Kinnison, D., Lamarque, J., Marsh, D.,
408 Mills, M. J., Tilmes, S., Bardeen, C., Buchholz, R. R., Conley, A., Gettelman, A., Garcia, R., Simpson,
409 I., Blake, D. R., Meinardi, S. and Pétron, G.: The chemistry mechanism in the community earth system
410 model version 2 (CESM2), J. Adv. Model. Earth Syst., 12(4), e2019MS001882, 2020.

411 Epstein, S. A., Riipinen, I. and Donahue, N. M.: A semiempirical correlation between enthalpy of
412 vaporization and saturation concentration for organic aerosol, Environ. Sci. Technol., 44(2), 743–748,
413 2010.

414 Gelaro, R., McCarty, W., Suárez, M. J., Todling, R., Molod, A., Takacs, L., Randles, C., Darmenov, A.,
415 Bosilovich, M. G., Reichle, R., Wargan, K., Coy, L., Cullather, R., Draper, C., Akella, S., Buchard, V.,
416 Conaty, A., da Silva, A., Gu, W., Kim, G.-K., Koster, R., Lucchesi, R., Merkova, D., Nielsen, J. E.,
417 Partyka, G., Pawson, S., Putman, W., Rienecker, M., Schubert, S. D., Sienkiewicz, M. and Zhao, B.:
418 The Modern-Era Retrospective Analysis for Research and Applications, Version 2 (MERRA-2), J.
419 Clim., 30(Iss 13), 5419–5454, 2017.

420 Gettelman, A., Hannay, C., Bacmeister, J. T., Neale, R. B., Pendergrass, A. G., Danabasoglu, G.,
421 Lamarque, J. -F, Fasullo, J. T., Bailey, D. A., Lawrence, D. M. and Mills, M. J.: High Climate
422 Sensitivity in the Community Earth System Model Version 2 (CESM2), Geophys. Res. Lett., 46(14),
423 8329–8337, 2019a.

424 Gettelman, A., Mills, M. J., Kinnison, D. E., Garcia, R. R., Smith, A. K., Marsh, D. R., Tilmes, S., Vitt,
425 F., Bardeen, C. G., McInerny, J., Liu, H.-L., Solomon, S. C., Polvani, L. M., Emmons, L. K., Lamarque,
426 J.-F., Richter, J. H., Glanville, A. S., Bacmeister, J. T., Phillips, A. S., Neale, R. B., Simpson, I. R.,
427 DuVivier, A. K., Hodzic, A. and Randel, W. J.: The whole atmosphere community climate model
428 version 6 (WACCM6), J. Geophys. Res., 124(23), 12380–12403, 2019b.

429 Goldstein, A. H. and Galbally, I. E.: Known and unexplored organic constituents in the earth's
430 atmosphere, Environ. Sci. Technol., 41(5), 1514–1521, 2007.

431 Guenther, A. B., Jiang, X., Heald, C. L., Sakulyanontvittaya, T., Duhl, T., Emmons, L. K. and Wang, X.:

The Model of Emissions of Gases and Aerosols from Nature version 2.1 (MEGAN2.1): an extended and updated framework for modeling biogenic emissions, Geoscientific Model Development, 5(6), 1471–1492, 2012.

Hallquist, M., Wenger, J. C., Baltensperger, U., Rudich, Y., Simpson, D., Claeys, M., Dommen, J., Donahue, N. M., George, C., Goldstein, A. H., Hamilton, J. F., Herrmann, H., Hoffmann, T., Iinuma, Y., Jang, M., Jenkin, M. E., Jimenez, J. L., Kiendler-Scharr, A., Maenhaut, W., McFiggans, G., Mentel, T. F., Monod, A., Prévôt, A. S. H., Seinfeld, J. H., Surratt, J. D., Szmigielski, R. and Wildt, J.: The formation, properties and impact of secondary organic aerosol: current and emerging issues, Atmos. Chem. Phys., 9(14), 5155–5236, 2009.

Hodzic, A., Kasibhatla, P. S., Jo, D. S., Cappa, C. D., Jimenez, J. L., Madronich, S. and Park, R. J.: Rethinking the global secondary organic aerosol (SOA) budget: stronger production, faster removal, shorter lifetime, Atmos. Chem. Phys., 16(12), 7917–7941, 2016.

Hodzic, A., Campuzano-Jost, P., Bian, H., Chin, M., Colarco, P. R., Day, D. A., Froyd, K. D., Heinold, B., Jo, D. S., Katich, J. M., Kodros, J. K., Nault, B. A., Pierce, J. R., Ray, E., Schacht, J., Schill, G. P., Schroder, J. C., Schwarz, J. P., Sueper, D. T., Tegen, I., Tilmes, S., Tsigaridis, K., Yu, P. and Jimenez, J. L.: Characterization of organic aerosol across the global remote troposphere: a comparison of ATom measurements and global chemistry models, Atmos. Chem. Phys., 20(8), 4607–4635, 2020.

Jo, D. S., Hodzic, A., Emmons, L. K., Marais, E. A., Peng, Z., Nault, B. A., Hu, W., Campuzano-Jost, P. and Jimenez, J. L.: A simplified parameterization of isoprene-epoxydiol-derived secondary organic aerosol (IEPOX-SOA) for global chemistry and climate models: a case study with GEOS-Chem v11-02-rc, Geoscientific Model Development, 12(7), 2983–3000, 2019.

Jo, D. S., Hodzic, A., Emmons, L. K., Tilmes, S., Schwantes, R. H., Mills, M. J., Campuzano-Jost, P., Hu, W., Zaveri, R. A., Easter, R. C., Singh, B., Lu, Z., Schulz, C., Schneider, J., Shilling, J. E., Wisthaler, A. and Jimenez, J. L.: Future changes in isoprene-epoxydiol-derived secondary organic aerosol (IEPOX SOA) under the Shared Socioeconomic Pathways: the importance of physicochemical dependency, Atmos. Chem. Phys., 21(5), 3395–3425, 2021.

Lana, A., Bell, T. G., Simó, R., Vallina, S. M., Ballabrera-Poy, J., Kettle, A. J., Dachs, J., Bopp, L., Saltzman, E. S. and Stefels, J.: An updated climatology of surface dimethylsulfide concentrations and emission fluxes in the global ocean, Global Biogeochem. Cycles, 25(1), 2011.

Lawrence, D. M., Fisher, R. A., Koven, C. D., Oleson, K. W., Swenson, S. C., Bonan, G., Collier, N., Ghimire, B., Kampenhout, L., Kennedy, D., Kluzek, E., Lawrence, P. J., Li, F., Li, H., Lombardozzi, D., Riley, W. J., Sacks, W. J., Shi, M., Vertenstein, M., Wieder, W. R., Xu, C., Ali, A. A., Badger, A. M., Bisht, G., Broeke, M., Brunke, M. A., Burns, S. P., Buzan, J., Clark, M., Craig, A., Dahlin, K., Drewniak, B., Fisher, J. B., Flanner, M., Fox, A. M., Gentine, P., Hoffman, F., Keppel-Aleks, G., Knox, R., Kumar, S., Lenaerts, J., Leung, L. R., Lipscomb, W. H., Lu, Y., Pandey, A., Pelletier, J. D., Perket, J., Randerson, J. T., Ricciuto, D. M., Sanderson, B. M., Slater, A., Subin, Z. M., Tang, J., Thomas, R.

22

468   Q., Val Martin, M. and Zeng, X.: The community land model version 5: Description of new features,
469   benchmarking, and impact of forcing uncertainty, J. Adv. Model. Earth Syst., 11(12), 4245–4287, 2019.

470   Liu, X., Easter, R. C., Ghan, S. J., Zaveri, R., Rasch, P., Shi, X., Lamarque, J.-F, Gettelman, A.,
471   Morrison, H., Vitt, F., Conley, A., Park, S., Neale, R., Hannay, C., Ekman, A. M. L., Hess, P.,
472   Mahowald, N., Collins, W., Iacono, M. J., Bretherton, C. S., Flanner, M. G. and Mitchell, D.: Toward a
473   minimal representation of aerosols in climate models: description and evaluation in the Community
474   Atmosphere Model CAM5, Geoscientific Model Development, 5(3), 709–739, 2012.

475   Liu, X., Ma, P.-L., Wang, H., Tilmes, S., Singh, B., Easter, R. C., Ghan, S. J. and Rasch, P. J.:
476   Description and evaluation of a new four-mode version of the Modal Aerosol Module (MAM4) within
477   version 5.3 of the Community Atmosphere Model, Geoscientific Model Development, 9(2), 505–522,
478   2016.

479   Robinson, A. L., Donahue, N. M., Shrivastava, M. K., Weitkamp, E. A., Sage, A. M., Grieshop, A. P.,
480   Lane, T. E., Pierce, J. R. and Pandis, S. N.: Rethinking organic aerosols: semivolatile emissions and
481   photochemical aging, Science, 315(5816), 1259–1262, 2007.

482   Schwantes, R. H., Lacey, F. G., Tilmes, S., Emmons, L. K., Lauritzen, P. H., Walters, S., Callaghan, P.,
483   Zarzycki, C. M., Barth, M. C., Jo, D. S., Bacmeister, J. T., Neale, R. B., Vitt, F., Kluzek, E., Roozitalab,
484   B., Hall, S. R., Ullmann, K., Warneke, C., Peischl, J., Pollack, I. B., Flocke, F., Wolfe, G. M., Hanisco,
485   T. F., Keutsch, F. N., Kaiser, J., Bui, T. P. V., Jimenez, J. L., Campuzano-Jost, P., Apel, E. C.,
486   Hornbrook, R. S., Hills, A. J., Yuan, B. and Wisthaler, A.: Evaluating the impact of chemical
487   complexity and horizontal resolution on tropospheric ozone over the conterminous US with a global
488   variable resolution chemistry model, J. Adv. Model. Earth Syst., doi:10.1029/2021ms002889, 2022.

489   Sporre, M. K., Blichner, S. M., Karset, I. H. H., Makkonen, R. and Berntsen, T. K.:
490   BVOC–aerosol–climate feedbacks investigated using NorESM, Atmos. Chem. Phys., 19(7),
491   4763–4782, 2019.

492   Srivastava, D., Vu, T. V., Tong, S., Shi, Z. and Harrison, R. M.: Formation of secondary organic aerosols
493   from anthropogenic precursors in laboratory studies, npj Climate and Atmospheric Science, 5(1), 1–30,
494   2022.

495   Tilmes, S., Hodzic, A., Emmons, L. K., Mills, M. J., Gettelman, A., Kinnison, D. E., Park, M.,
496   Lamarque, J. -F, Vitt, F., Shrivastava, M., Campuzano-Jost, P., Jimenez, J. L. and Liu, X.: Climate
497   Forcing and Trends of Organic Aerosols in the Community Earth System Model (CESM2), J. Adv.
498   Model. Earth Syst., 18, 17,745, 2019.

499   Tsigaridis, K. and Kanakidou, M.: The Present and Future of Secondary Organic Aerosol Direct Forcing
500   on Climate, Current Climate Change Reports, 4(2), 84–98, 2018.

501   Wang, S., Hornbrook, R. S., Hills, A., Emmons, L. K., Tilmes, S., Lamarque, J., Jimenez, J. L.,

502 Campuzano-Jost, P., Nault, B. A., Crounse, J. D., Wennberg, P. O., Kim, M., Allen, H., Ryerson, T. B.,
503 Thompson, C. R., Peischl, J., Moore, F., Nance, D., Hall, B., Elkins, J., Tanner, D., Huey, L. G., Hall, S.
504 R., Ullmann, K., Orlando, J. J., Tyndall, G. S., Flocke, F. M., Ray, E., Hanisco, T. F., Wolfe, G. M., St.
505 Clair, J., Commane, R., Daube, B., Barletta, B., Blake, D. R., Weinzierl, B., Dollner, M., Conley, A.,
506 Vitt, F., Wofsy, S. C., Riemer, D. D. and Apel, E. C.: Atmospheric Acetaldehyde: Importance of Air-Sea
507 Exchange and a Missing Source in the Remote Troposphere, Geophys. Res. Lett., 46(10), 5601–5613,
508 2019.

509 Wang, S., Apel, E. C., Schwantes, R. H., Bates, K. H., Jacob, D. J., Fischer, E. V., Hornbrook, R. S.,
510 Hills, A. J., Emmons, L. K., Pan, L. L., Honomichl, S., Tilmes, S., Lamarque, J.-F., Yang, M.,
511 Marandino, C. A., Saltzman, E. S., de Bruyn, W., Kameyama, S., Tanimoto, H., Omori, Y., Hall, S. R.,
512 Ullmann, K., Ryerson, T. B., Thompson, C. R., Peischl, J., Daube, B. C., Commane, R., McKain, K.,
513 Sweeney, C., Thames, A. B., Miller, D. O., Brune, W. H., Diskin, G. S., DiGangi, J. P. and Wofsy, S. C.:
514 Global atmospheric budget of acetone: Air-sea exchange and the contribution to hydroxyl radicals, J.
515 Geophys. Res., 125(15), doi:10.1029/2020jd032553, 2020.

516 Warneck, P. and Williams, J.: The Atmospheric Chemist's Companion, Springer Dordrecht., 2012.